Structural Basis of Stress Concentration in the Cytoskeleton

Ning Wang[*]

Abstract: Professor Y.C. Fung has shown that living tissues remodel extensively in response to mechanical forces such as blood pressure variations. At the cellular level, those mechanical perturbations must be perceived by individual cells. However, mechanisms of mechanochemical transduction in living cells remain a central challenge to cell biologists. Contrary to predictions by existing models of living cells, we reported previously that a local stress, applied via integrin receptors, is propagated to remote sites in the cytoplasm and is concentrated at discrete foci. Here we report that these foci of strains and stresses in the cytoplasm correspond to local peak deformation or local buckling of microtubules and are near the actin bundles of the cell. Multiple images at different z heights demonstrated more foci of concentrated displacements in the middle of the cell than at the apex or at the cell base. Together with previously published work, these findings underscore the importance of tensed bundled filamentous actin in intracellular mechanical stress distribution and signaling.

Keyword: microtubules, actin bundles, mechanical deformation, integrins

1 Introduction

Professor Y. C. Fung has pioneered the work of tissue remodeling in response to mechanical forces and introduced the concept of zero-stress state (1, 2). The remodeling of the tissues must come from the responses of the living cells and it is well known that mechanical forces are critical for regulating vital cell functions. However, the mechanism of mechanotransduction, i.e., how and where mechanical forces are transduced into biochemical activities and biological responses in a living cell, remains largely unknown (3-8). During the last decade or so, integrins and focal adhesions were shown to play essential roles in mediating force transmission and transduction across the cell surface into the cytoplasm (9-14). In a conventional continuum material, the magnitudes of a local applied force decrease as the square of the distance from the force impact. Therefore it is widely accepted that applied local forces are mostly dissipated at the focal adhesions on the cell surface (15) such that there should be little direct deep cytoplasmic deformation and no direct nuclear deformation beyond the close vicinity of the applied force. This view is supported by the finite element analysis of cell models based on principles of continuum mechanics (16). In sharp contrast, we have demonstrated that a local load of physiologic magnitudes applied at the cell apical surface via integrin receptors is propagated along the cytoskeleton (CSK) to remote sites in the cytoplasm (17) and into the nucleus (18). Importantly, strains are concentrated at discrete sites deep in the cytoplasm and inside the nucleolus (17-19), tens of micrometers away from the site of load application at the apical surface. These findings represent a major departure from predictions of existing models of living cells and challenge the prevailing views on mechanical signaling inside a living cell. Importantly, our recent work shows that this long-distance force propagation to the deep cytoplasm is crucial in rapidly activating Src protein in those remote sites (20). Therefore, the strain focusing in the cytoplasm is necessary for rapid and remote mechanotransduction. In this study, we present direct experimental evidence for the structural basis of the observed strain concentration in the CSK of a living cell.

[*] Department of Mechanical Science and Engineering, University of Illinois at Urbana-Champaign, 1206 W. Green St., Urbana, IL 61801 USA. Tel: 217-265-0913 (o), 217-333-1942 (f); Email: nwangrw@uiuc.edu

2   Results

We applied local oscillatory stresses to a living cell via integrin receptors using a ∼4-μm RGD-coated magnetic bead. The bead bound specifically to integrin receptors on the apical surface (9) and induced local focal adhesions that physically connected to the actin CSK (Fig. 1). Previously, using YFP(yellow fluorescent protein)-mitochondria as markers of the CSK, we demonstrated that strains and stresses were concentrated at sites deep in the cytoplasm from the load (17). Because mitochondria are not direct stress-bearing elements in the cytoplasm, it is very difficult to elucidate the structural basis of strain concentration from maps of YFP-mitochondria displacements. Therefore in this study we directly quantified the displacements/deformation of the CSK by using GFP(green fluorescent protein)-tubulin or YFP-actin transfected cells.

The cell transfected with GFP-tubulin exhibited synchronous displacements in the deep cytoplasm in response to an oscillatory loading (at 0.83 Hz) via the RGD-bead (Fig. 2a, 2b). We define the site of strain concentration/focusing as a point at which a local peak deformation/displacement is at least 30% greater than the surrounding deformation/displacements. Overlapping the displacement map with the fluorescent map of the same cell, we found numerous strain focusing sites in the cell (Fig. 2d; each blue circle represents a strain focusing site). The number of strain focusing sites increased with the extent of the overall cell surface deformation at focal adhesions (not shown). Comparing microtubule (MT) fluorescent images before and during peak loading, we observed that local peak displacements/deformation of MT coincided with the sites of strain focusing (Fig. 2c). Interestingly, local MT buckling sites were found to overlap with the sites of strain concentration (Fig. 2c). Using the stiffness measured via the magnetic bead as an approximate of the average cell stiffness, we generated the stress map of the MT in response to the applied stress (Fig. 2e). The stress map shows that the stresses were also focused at sites away from the loading site.
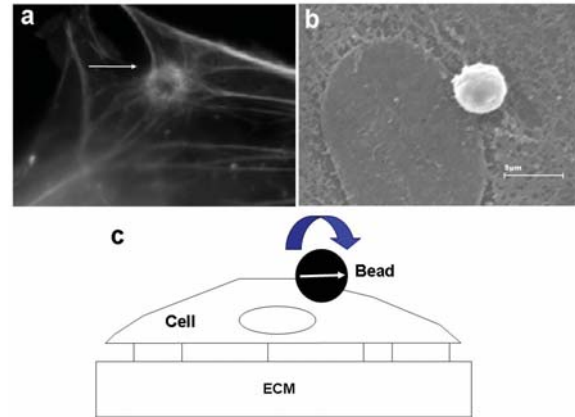
Figure 1: Loading a single living cell locally via integrin receptors. (a) An Arg-Gly-Asp (RGD)-peptides coated ferromagnetic bead (4.5 μms in diameter) (white arrow) was bound to the apical surface of a live smooth muscle cell transfected with YFP-actin. Note the abundant F-actin near the bead surface and numerous actin bundles. (b) A transmission electron microscopy image of a RGD-coated magnetic bead next to the nucleus. Note the appearance of cytoskeletal filaments of different sizes. Scale bar=5 μms. (c) Schematic of load application via the oscillatory torque (blue arrow) to a magnetized bead (white arrow) bound to a spread cell adherent to a collagen-1 coated surface.

Since the actin filament network is the first CSK filament system to experience mechanical stresses downstream from the focal adhesions, we mapped displacements and stresses of the YFP-actin cell in response to the applied stress via the magnetic bead (Fig. 3a). It is apparent that the displacements (Fig. 3b) and stresses (Fig. 3d) were both propagated to remote cytoplasmic sites in addition to the local vicinity of the loading site. Interestingly, when the fluorescent map and the displacement maps were overlapped, the majority of the numerous strain focusing sites (the blue circles) appear to be close to the actin bundles (Fig. 3c). These findings demonstrate that actin bundles are the most likely candidates for transmitting stresses to long distances along the long axis of the actin bundles to deform other CSK filaments such as the MTs and to result in strain fo-
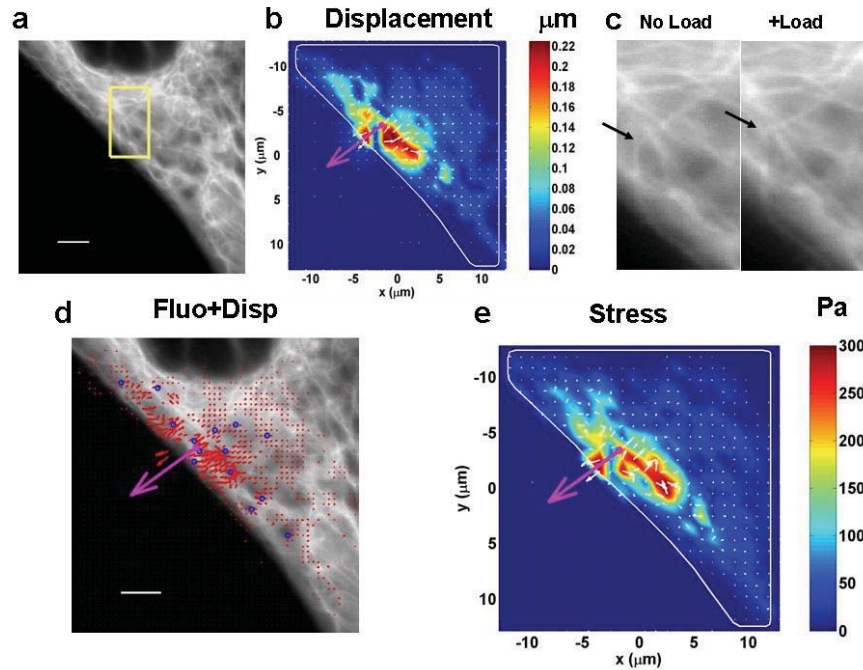
Figure 2: Local microtubule maximum deformation corresponds to straining focusing sites. (a) A representative live GFP-tubulin smooth muscle cell image at $\sim$2 μm above the cell base. The black area on the top middle is part of the nucleus. (b) The peak displacement map of the same cell in response to an oscillatory loading via a RGD-coated magnetic bead (26.3 Pa at 0.3 Hz). (c) The buckling of a microtubule in the presence of peak loading (right image) when compared with the much less buckled microtubule in absence of the peak load (left image). This region corresponds to the blown-up area of the yellow rectangular in (a). Note the buckling point of the microtubule (black arrow in right image) corresponds exactly to the strain focusing point (a small blue circle) in (d). (d) Overlapping the fluorescent image and the displacement map (Fluo+Disp) of the microtubule network reveals numerous strain focusing sites (small blue circles) in response to loading. (e) The computed stress map of the microtubule network based on the displacement map and the estimated average cell stiffness. The pink arrow in (b), (d), and (e) represents the position of the bead center and the direction of the bead center movement. The colors represent the magnitudes of displacements or stresses. The scale bar is 5 μm. Four other cells exhibited similar behaviors.

cusing in MTs.

To obtain a more precise picture how stresses are propagated from the apical surface to the basal surface, we performed multiple z-scans for a single cell transfected with GFP-MT, YFP-actin, or YFP-mitochondria while stressing the cell at a given sinusoidal frequency of 0.83 Hz. Then we stacked the fluorescent images to obtain a 3D image of the CSK (left images of Fig. 4). Multiple x-y displacement images were stacked together to construct a 3D image of the displacements in the x-y plane (right images of Fig. 4). We found that the displacements were heterogeneous throughout the height of the cell (Fig. 4a, 4b, 4c), with-

out much decay in magnitudes, consistent with our data from a single focal plane. By overlapping fluorescent images with the local concentrated displacements, we found that the distribution and number of displacement concentrations varied with cell height: there were more concentration sites in the middle of the cytoplasm than at the cell base or at the cell apex (Fig. 5a, 5b, 5c), raising intriguing questions about the possibility of activating numerous biomolecules in the deep cytoplasm.
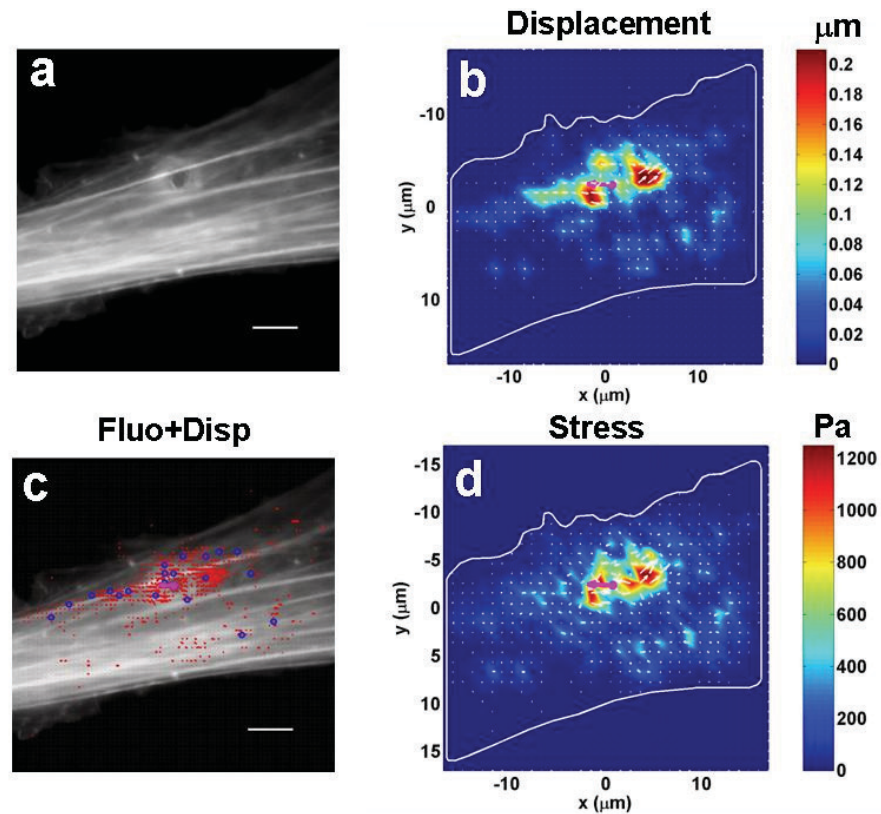
Figure 3: A YFP-actin smooth muscle cell responds to a localized load (75 gauss at 0.3 Hz). (a) The YFP-actin fluorescent image of the cell (at ∼1.5 μms above the cell base) showing numerous actin bundles/stress fibers. The dark spot at the top middle of the image is the RGD-bead. Note the accumulation of YFP-actin surrounding the bead. (b) The displacement map of the cell. White arrows represent the direction and relative magnitudes of the displacements. Colors represent the magnitudes of displacements. (c) Overlapping of the fluorescent image and the displacement map. Red arrows represent the relative magnitudes and directions of displacements. Small blue circles represent the sites of strain focusing. (d) The computed stress map of the cell. White arrows and colors represent the directions and magnitudes of the stresses. Pink arrow represents the location and direction of the magnetic bead center displacement. Scale bar=5 μm. Two other cells exhibited similar behaviors.

3   Discussion

We have demonstrated that local maximum displacements/deformation sites of microtubules are the sites of stress/strain concentration. Living cells exhibit heterogeneous strain distribution throughout the cytoplasm of the cell in response to a localized load application.

The goal of the present study is to determine the structural basis of strain/stress focusing in the cytoplasm by directly quantifying CSK filament displacements and deformation, rather than using mitochondria as a surrogate of CSK displacements. We previously demonstrated strain/stress focusings in the cytoplasm of individual living cells in response to a localized stress application (17-19). However, due to the fact that mitochondria are not major stress-bearing elements, lack of structural information on stress-bearing elements in the cytoplasm makes it difficult to determine the structural mechanism of stress/strain concentration. Another limitation of using mitochondria for markers of CSK filaments is that the density of mitochondria determines how many displacement data can be tracked and measured. Thus it is likely that using YFP-mitochondria to map CSK

(a)

(b)

(c)
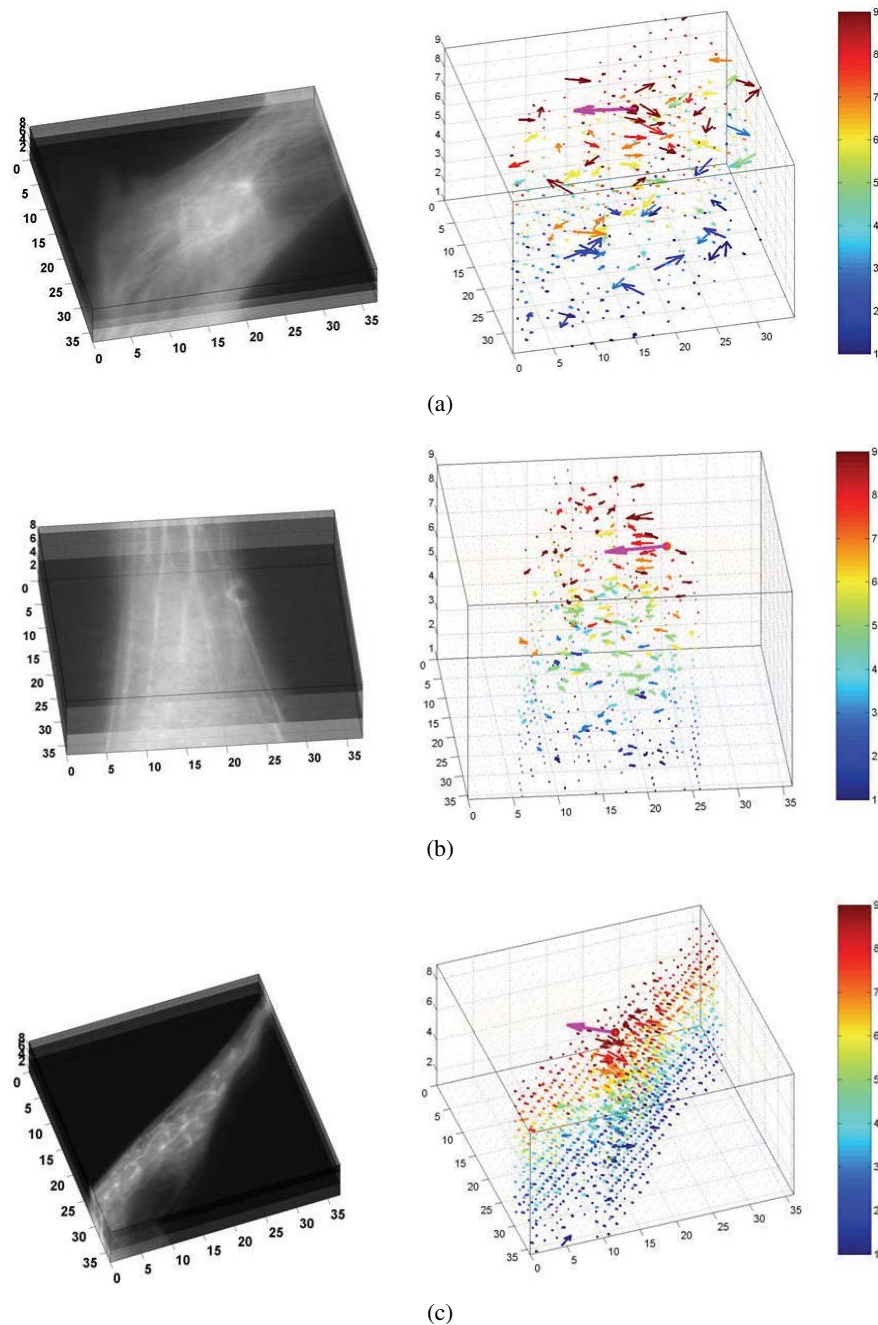
Figure 4: (a) 3D fluorescent image (left) and stacked 2D displacement map (right) of GPF-tubulin of a live smooth muscle cell in response to a localized load (17.5 Pa at 0.83 Hz). Color arrows represent positions, local directions, and relative magnitudes of the displacements at each focal plane from bottom to top (dark blue to dark red). The pink arrow represents the position, direction, and relative magnitude of the magnetic bead center displacement. The number in the z–axis represents each focal plane at 0.5 μm apart. Scale in x and y axis is in μm. For visual clarity, only one out of every two displacements is plotted. (b) 3D fluorescent image (left) and stacked 2D displacement map (right) of YFP-actin of a live smooth muscle cell in response to a localized load (17.5 Pa at 0.3 Hz). The half white circle of YFP-actin in the fluorescent image is the position of the magnetic bead. The notations are the same as in Fig. 4a. (c) 3D fluorescent image (left) and stacked 2D displacement map (right) of YPF-mitochondria of a live smooth muscle cell in response to a localized load (17.5 Pa at 0.3 Hz). The notations are the same as in Fig. 4a.
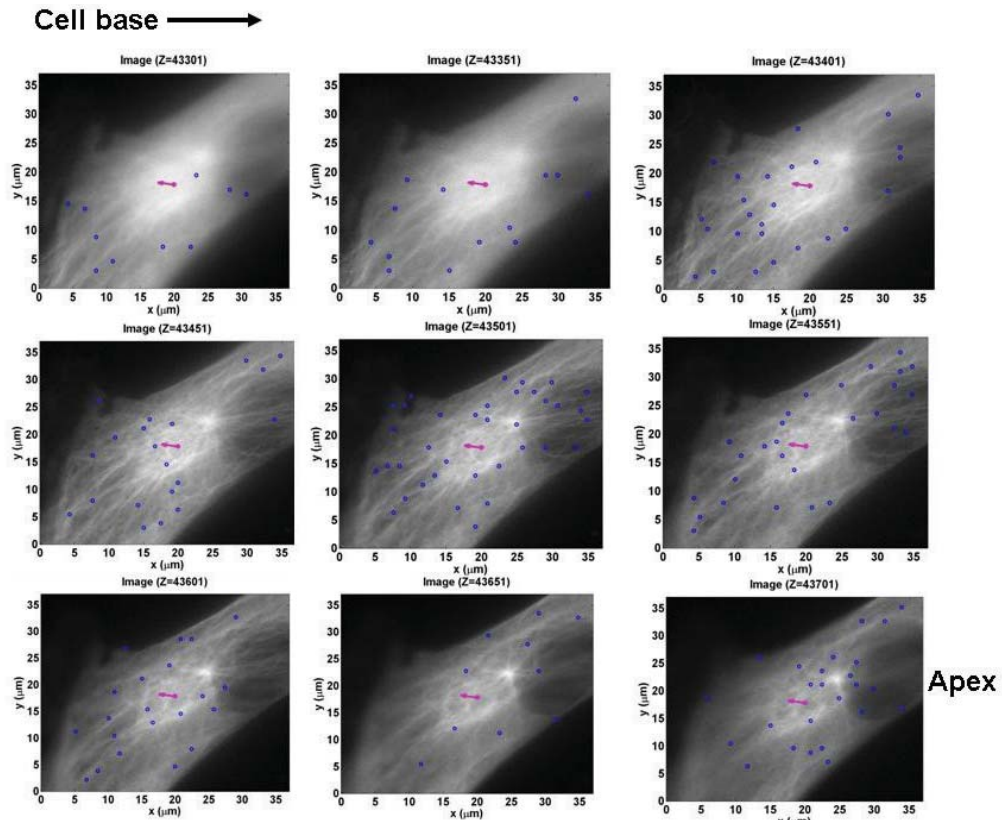
(a)
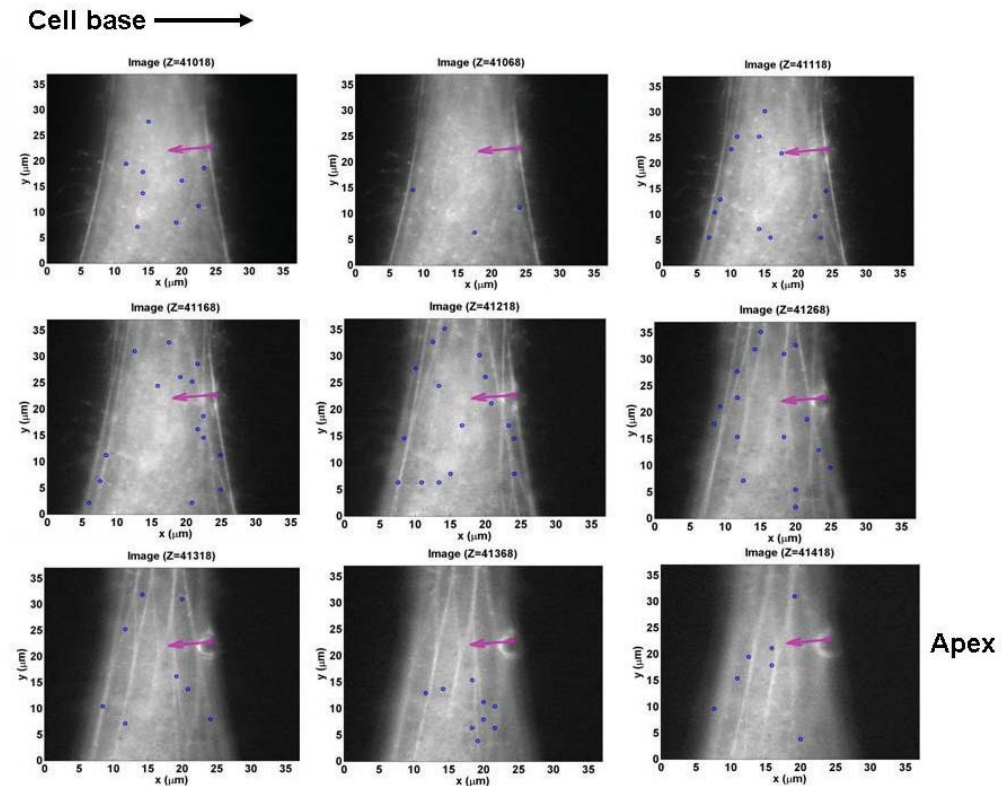
(b)
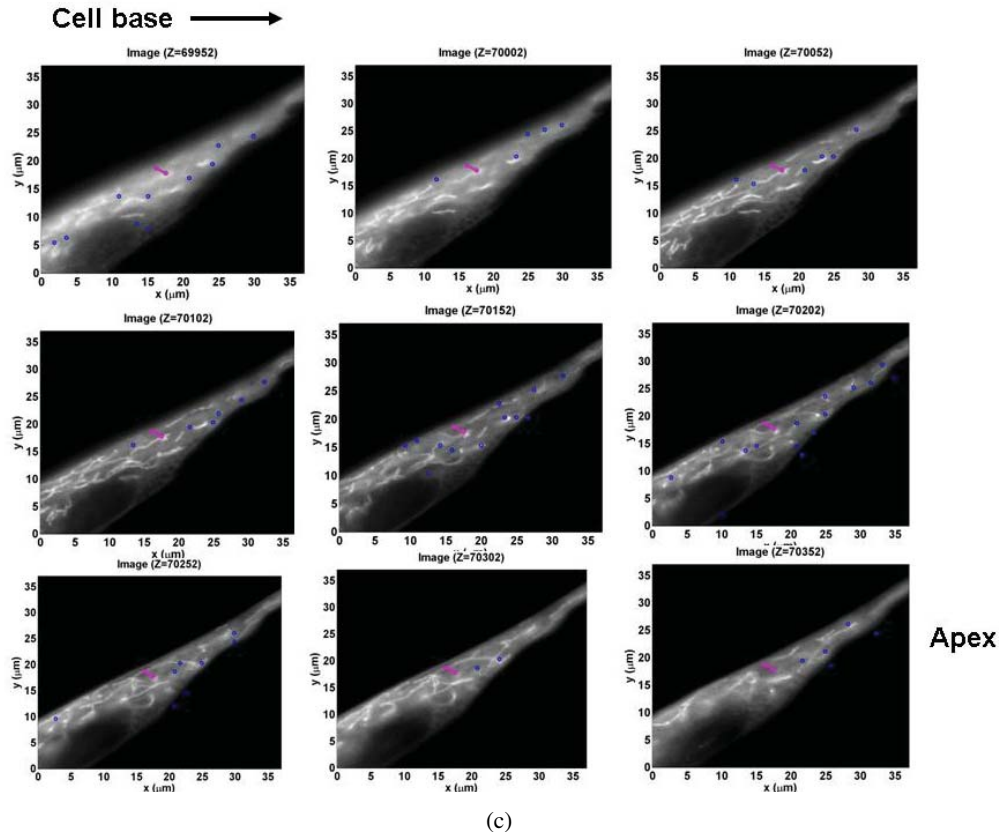
Figure 5: (a) The number of microtubule displacement concentrations varies as a function of cell height. Multiple GFP-tubulin fluorescent images were taken from cell base to apex at 0.5 μm per slice. Blue circles represent sites of local peak displacements that are at least 30% greater than the surrounding displacements. Pink arrow represents the direction and position of the magnetic bead. Clearly there are more blue circles in the middle of the cytoplasm than at cell base or cell apex. These images correspond to Fig. 4a. (b) The number of F-actin displacement concentrations varies as a function of focal planes. Multiple YFP-actin fluorescent images were taken from cell base to apex at 0.5 μm per slice. Blue circles represent sites of local peak displacements that are at least 30% greater than the surrounding displacements. Pink arrow represents the direction and position of the magnetic bead. There appear to be more blue circles in the middle of the cytoplasm than at cell base or cell apex. These images correspond to Fig. 4b. (c) The number of mitochondria displacement concentrations varies as a function of focal planes. Multiple YFP-mitochondria fluorescent images were taken from cell base to apex at 0.5 μm per slice. Blue circles represent sites of local peak displacements that are at least 30% greater than the surrounding displacements. Pink arrow represents the direction and position of the magnetic bead. There are more blue circles in the middle of the cytoplasm than at cell base or cell apex. These images correspond to Fig. 4c.

displacements may underestimate the number of strain/stress focusing in a cell.

Since it is difficult to precisely quantify z displacements in a living cell, all our present data in a single focal plane or in multiple focal planes have only displacements in x-y plane. However, lack of z-displacements will not change our conclusion about the structural basis of strain focusing. Importantly, all the cells are well spread and the local applied strains are relatively small, hence any induced z displacements would be small (relative to x and y displacements) and might not contribute significantly to the total displacements except at the close vicinity of the magnetic bead.

Our data suggest that the structural basis for the strain/stress focusing in the cytoplasm measured via YFP-mitochondria markers in previous reports appears to be the local peak deformation of the MTs. What is the relationship between strain focusings of the MTs and strain focusings of microfilaments (MFs)? At the present time, we do not have definitive answers to this question, because it is difficult to obtain precise maps of displacements of MT and MF separately in the same cell. However, the stresses are transmitted at cell surface from integrins to the F-actin and from the F-actins to MTs via MACF1 (microtubule actin crosslinking factor) (21). Thus, any displacements, especially concentrated displacements in MTs should depend on the concentrated stresses from MFs, especially actin bundles. This explanation is consistent with our previous findings that tensed actin bundles mediate long distance force transmission in the cytoplasm(17, 19) and consistent with the report that in migrating cells MTs are buckled by converging actin bundles(22).

Based on the principle of mechanical equilibrium, any applied shear stresses at the apical cell surface must be balanced by structures at the cell base, namely, at the basal adhesions. Otherwise, the whole cell will be detached or removed from the substrate by the applied shear stress. The focal adhesions are concentration sites of integrins, CSK structures (e.g., actin bundles and/or stress fibers), and linking proteins (e.g., talin, vinculin, and paxillin, etc). Existing models of single living cells predict that a local force is balanced by basal focal adhesion sites in the close vicinity of the loading site, since stresses decay in space approximately in proportion to the square of the distance from the loading site. However, we have recently shown that applied stresses at the apical surface of the cell are propagated to cytoplasmic sites far way (many tens of μms away) (17-19). These findings raise an important question in mechanotransduction: can one just look for local activities (either mechanical or biochemical), or must one also look for remote site activities, in response to a local force applied at a focal adhesion? The answer appears to be the latter, based on our recent experimental findings (20). More-

over, the concentrated deformations in the cytoplasm far away from the applied force pose the challenge as to how a living cell integrates these mechanical signals with soluble factor signals inside the cytoplasm.

Cell membranes are the first sites to experience mechanical forces and have been proposed early on as the primary stress-bearing elements in response to externally applied surface stresses. However, experiments in various cell types have shown that the CSK is the primary stress-bearing elements (9, 23). The most effective way to deform the CSK via the cell surface is through the cell-matrix adhesion molecule integrins. Taken together with the earlier report that nonadhesion molecules did not mediate long-distance deformation in the CSK (24), the current finding that the strain/stress focusings are along the actin bundles and occur at sites where local maximal MT displacements and deformation happen suggests that long distance propagation of stresses is a unique mechanical signaling pathway via adhesion molecules. In addition, the actin bundles must be prestressed or tensed in order for stresses to be propagated rapidly and remotely (17-19) to activate cytoplasmic proteins (20). The stresses are propagated along preferred structural pathways by the elastic wave propagation mechanism such that it takes much less than 1 ms for a local force to reach the nucleus and the cytoplasmic sites inside the cell from the cell surface (20).

Microtubules can bend and buckle under endogenous CSK tension (22, 24) or external forces (25, 26). However, microtubules are reinforced by lateral filaments in living cells such that it takes much higher external stresses to buckle a single MT in a living cell than in isolated MT (26). Our present results are consistent with these published reports: the load applied via the magnetic bead buckled only a few MTs whereas the majority of the MTs only exhibit displacements/deformation without buckling. In contrast, many more MTs are buckled or broken during cell migration in response to very large endogenous CSK stresses (22).

The previous findings on the weak dependence of cell elastic modulus on loading frequency (the

weak power law) (27, 28) attract much attention to the dynamics of the CSK in response to applied stresses. Recently, it is demonstrated, however, that at lower frequencies (0.001-0.1), there is another power law with a different slope, suggesting that multi power laws exist in living cells (29). Moreover, we have found that the response of stress propagation to loading frequency is biphasic: the maximal deformed areas for a given magnitude of load are at a loading frequency of ∼1 Hz for these airway smooth muscle cells (30). These data are consistent with in vivo studies in mice that optimal loading frequencies for bone adapdation are at 5-10 Hz (31). In the present study we employed a loading frequency of 0.83 Hz or 0.3 Hz to maximize the effect of loading on the mechanical stress propagation.

4 A working model of stress propagation in the cytoplasm

Our current working model of stress propagation and mechanotransduction: Stresses applied via integrin adhesion sites are propagated via the focal adhesions to the actin CSK; from there, forces are propagated via tensed actin bundles to MTs and intermediate filaments (32) to remote sites in the cytoplasm; along the pathway, local biochemical activities of individual molecules in cytosol, in the nucleus, and/or associated with the CSK are modulated and altered by these propagating stresses. This model is supported by our recent experimental evidence that Src proteins anchored on the membranes of endosomes are activated only when MTs are deformed, which, in turn, leads to endosomal membrane deformation (20). The MTs are deformed at remote sites only when propagating stresses along the tensed actin bundles reached these MTs. This signaling pathway, together with mechanotransduction induced by stretch-dependent ion channels in the plasma membrane and by the local activation of focal adhesion proteins, may help facilitate the integrated biochemical and biological responses of the cell to mechanical stresses. Eventually, these cellular reponses will be translated into remodeling of the extracellular matrix and remodeling of the living tissues (1, 2).

5 Methods and Materials

Cell Culture Human airway smooth muscle cells (HASM) were isolated and cultured as previously described (17). Cells at passage 3-8 were used for all experiments. These cells still maintain smooth muscle cell morphology and physiological responsiveness to agonists at passage 8. After cells reached confluence in culture dishes, they were serum deprived for 24 h before being trypsinized. Following trypsinization, cells were plated in serum free medium overnight in 35-mm dishes for displacement measurements. HASM cells did not enter cell cycle but maintained contractile profile in serum-free medium. The 35-mm dishes were pre-coated with collagen-1 (0.2 mg/ml). Then the cells were plated in the wells at 10,000 cells/dish.

Adenovirus Transfection Assay The adenovirus fluorescent protein assay was developed and used following protocols described previously (17). After the cells reached 70-80% confluency, the adenovirus-containing YFP-actin, GFP-tubulin, or YFP-mitochondria were added at 150 μl per well (6-well dish) for 2 days and transfection efficiency was examined under the fluorescent microscope.

Microscopy We used an inverted microscope (Leica) with a 40X objective (one pixel = 160 nm) or with a 63X oil objective (one pixel = 101 nm). The ambient vibration was prevented using a vibration isolation table (Newport, Irvine, CA). A progressive scan, triggerable black and white charge-coupled device camera with pixel-clock synchronization (Hamamatsu, C4742-95-12ERG) was attached to the camera side-port of the microscope via a camera adapter. Image acquisition (50 ms per image) is phase locked to the sinusoidal twisting field.

Optical Magnetic Twisting Cytometry Optical magnetic cell twisting is an extension of the magnetic cell twisting technique (9) to oscillatory forcing. The technique of applying twisting torques to cells in a dish under a microscope had been described in detail (33). The microscope stage was heated to maintain 37°C for the cells in a dish. The twisting current was driven by a cur-

rent source controlled by a computer. Ferromagnetic beads (∼4 μm diameter) coated with saturated amount of Arg-Gly-Asp (RGD)-containing peptides (the ligand density on the bead was measured to be about 1 RGD-peptide per 3 nm^2 of bead surface area), ligands for integrin receptors, were bound the surface of the adherent HASM cells for 15 min. The binding specificity of bead binding was determined following protocols described previously (9). The magnetic moments of each batch of self-made ferromagnetic beads were calibrated according to published methods (9). A twisting field of 50 or 75 Gauss correspond to an apparent stress of 17.5 or 26.3 Pa. The beads are magnetized by a strong (1,000 G) and short (<0.1 ms) magnetic field pulse oriented at the horizontal direction using the magnetizing coils. A sinusoidally varying vertical magnetic "twisting" field is applied, and resulting bead translational displacements induced by bead rotation is determined by quantifying the bead center movement using an intensity-weighted-center-of-mass algorithm (33).

Image Processing Image acquisition was phase-locked to the twisting field such that 10 images were taken during one twisting cycle. To reduce noise caused by spontaneous cytoskeletal movements, images were taken during the same twisting phase over 3-10 cycles. The averaged images were cropped to a size of 32-μm square. The images were then subdivided into arrays of 11x11 pixels (2.2 μm × 2.2 μm). The arrays overlapped by 5 pixels. The deformation field was obtained by comparing corresponding arrays between two images taken at different phases during the twisting cycle. We shifted the arrays of the second image by sub-pixel increments (4 nm) in the Fourier-domain until the mean square differences of the pixel-intensities between the shifted array and the corresponding array from the first image reached a minimum. The resolution of the displacements was ∼5 nm (17, 19).

References

1. Fung YC, Liu SQ. (1991) Changes of zero-stress state of rat pulmonary arteries in hypoxic hypertension. *J Appl Physiol.* 70: 2455-70.

2. Li Z, Huang W, Jiang ZL, Gregersen H, Fung YC (2004) Tissue remodeling of rat pulmonary arteries in recovery from hypoxic hypertension. *Proc Natl Acad Sci U S A.* 101:11488-93.

3. Discher DE, Janmey P, Wang YL (2005) Tissue cells feel and respond to the stiffness of their substrate. *Science* 310:1139-1143.

4. Ingber DE (2006) Cellular mechanotransduction: putting all the pieces together again. *FASEB J* 20:811-827.

5. Giannone G, Sheetz MP (2006) Substrate rigidity and force define form through tyrosine phosphatase and kinase pathways. *Trends Cell Biol* 16:213-223.

6. Bershadsky, A, Kozlov M, Geiger B (2006) Adhesion-mediated mechanosensitivity: a time to experiment, and a time to theorize. *Curr. Opin. Cell Biol.* 18:472-81.

7. Orr AW, Helmke BP, Blackman BR, Schwartz MA (2006) Mechanisms of mechanotransduction. *Dev Cell* 10:11-20.

8. Janmey PA, McCulloch CA (2007) Cell mechanics: integrating cell responses to mechanical stimuli. *Annu Rev Biomed Eng* 9:1-34.

9. Wang N, Butler JP, Ingber DE (1993) Mechanotransduction across the cell surface

and through the cytoskeleton. *Science* 260: 1124-1127.

10. Choquet D, Felsenfeld DP, Sheetz MP (1997) Extracellular matrix rigidity causes strengthening of integrin-cytoskeleton linkages. *Cell* 88: 39-48.

11. Chicurel ME, Singer RH, Meyer CJ, Ingber DE (1998) Integrin binding and mechanical tension induce movement of mRNA and ribosomes to focal adhesions. *Nature* 392: 730-733.

12. Balaban NQ *et al.* (2001) Force and focal adhesion assembly: a close relationship studied using elastic micropatterned substrates. *Nat. Cell Biol*. 3: 466-472.

13. Wang Y *et al.* (2005) Visualizing the mechanical activation of Src. *Nature* 434:1040-1045.

14. Sawada Y *et al.* (2006) Force sensing by mechanical extension of the Src family kinase substrate p130Cas. *Cell* 127:1015-1026.

15. Vogel V, Sheetz MP (2006) Local force and geometry sensing regulate cell functions. *Nat Rev Mol Cell Biol* 7:265-275.

16. Mijailovich SM, Kojic M, Zivkovic M, Fabry B, Fredberg JJ (2002) A finite element model of cell deformation during magnetic bead twisting. *J. Appl. Physiol*. 93:1429-1436.

17. Hu S *et al.* (2003) Intracellular stress tomography reveals stress focusing and structural anisotropy in the cytoskeleton of living cells. *Am. J. Physiol. Cell Physiol.* 285: C1082-C1090.

18. Hu S, Chen J, Butler JP, Wang N (2005) Prestress mediates force propagation into the nucleus. *Biochem Biophys Res. Commu. 329:423-428.*

19. Hu S *et al* (2004) Mechanical anisotropy of adherent cells probed by a three dimensional magnetic twisting device. *Am. J. Physiol. Cell Physiol.* 287: C1184-C1191.

20. Na S *et al.* (2008) Rapid signal transduction in living cells is a unique feature of mechanotransduction. *Proc. Natl. Acad. Sci. U S A.* 105: 6626-6631.

21. Lin CM, Chen HJ, Leung CL, Parry DA, Liem RK. (2005) Microtubule actin crosslinking factor 1b: a novel plakin that localizes to the Golgi complex. *J Cell Sci.* 118:3727-38.

22. Gupton SL, Salmon WC, Waterman-Storer CM (2002) Converging populations of F-actin promote breakage of associated microtubules to spatially regulate microtubule turnover in migrating cells. *Curr. Biol.* 12: 1891-1899.

23. Trickey, W.R., T.P. Vail, and F. Guilak. 2004. The role of the cytoskeleton in the viscoelastic properties of human articular chondrocytes. *J. Orthop. Res*. 22: 131-9.

24. Wang N (2001) Mechanical behavior in living cells consistent with the tensegrity model. *Proc. Natl. Acad. Sci. USA* 98: 7765-7770.

25. Schaap IA, Carrasco C, de Pablo PJ, MacKintosh FC, Schmidt CF (2006) Elastic response, buckling, and instability of microtubules under radial indentation. *Biophys. J.* 91:1521-31.

26. Brangwynne CP *et al.* (2006) Microtubules can bear enhanced compressive loads in living cells because of lateral reinforcement. *J. Cell Biol.* 173:733-41.

27. Fabry B *et al*. (2001) Scaling the microrheology of living cells. *Phys. Rev. Lett.* 87:148102.

28. Deng LX *et al*. (2006) Fast and slow dynamics of the cytoskeleton. *Nat Mater.* 5:636-40.

29. Stamenoviæ D *et al*. (2007) Rheological behavior of living cells is timescale dependent. *Biophys J.* 93:L39-41.

30. Hu S, Wang N (2006) Control of stress propagation in the cytoplasm by prestress and loading frequency. *Mol. Cell Biomech*. 3:49-60.

31. Warden, S.J., and C.H. Turner. 2004. Mechanotransduction in the cortical bone is most efficient at loading frequencies of 5-10 Hz. *Bone* 34:261-70.

32. Wang N, Stamenovic D (2000) Contribution of intermediate filaments to cell stiffness, stiffening, and growth. *Am. J. Physiol. Cell Physiol.* 279: C188-C194.

33. Fabry B *et al*. (2001) Time course and hero-geneity of contractile responses in cultured human airway smooth muscle cells. *J. Appl. Physiol.* 91: 986-994.